

SciSat-1 Retrieval Results

Chris Boone*, Ray Nassar, Sean McLeod, Kaley Walker, and Peter Bernath
Department of Chemistry, University of Waterloo

ABSTRACT

SciSat-1, otherwise known as the Atmospheric Chemistry Experiment (ACE), is a Canadian satellite mission for remote sensing of the Earth's atmosphere. It was launched into low Earth orbit (altitude 650 km, inclination 74°) in August 2003. The primary instrument onboard ACE is a high resolution (maximum path difference ± 25 cm) Fourier Transform Spectrometer (FTS) operating from 2.4 to 13.3 microns ($750\text{--}4100\text{ cm}^{-1}$). The satellite also features a dual spectrograph known as MAESTRO with wavelength coverage 280-1000 nm and resolution 1-2 nm. A pair of filtered CMOS detector arrays takes images of the sun at 0.525 and 1.02 nm. Working primarily in solar occultation, the satellite provides altitude profile information for temperature, pressure, and the volume mixing ratios for several dozen molecules of atmospheric interest. Scientific goals for ACE include: (1) understanding the chemical and dynamical processes that control the distribution of ozone in the stratosphere and upper troposphere; (2) exploring the relationship between atmospheric chemistry and climate change; (3) studying the effects of biomass burning in the free troposphere; and (4) measuring aerosols to reduce the uncertainties in their effects on the global energy balance.

Keywords: remote sensing, occultation spectroscopy, geophysical parameter retrieval, ozone

1. INTRODUCTION

The Atmospheric Chemistry Experiment (ACE), officially designated SciSat-1, is the first in a planned series of small science satellites to be flown by the Canadian Space Agency. The satellite was successfully launched into low Earth orbit (650 km altitude) on August 12th, 2003. Following several months of commissioning activities, the satellite was declared operational for science measurements in late February, 2004. Since then, the instruments on the satellite have been monitoring the Earth's atmosphere from orbit. The measurements should provide insight into ozone depletion mechanisms,¹ biomass burning,² climate-chemistry coupling,³ and the effects of aerosols on the global energy balance.⁴

The primary instrument on board the satellite is a custom built Fourier transform spectrometer (FTS) operating between 2.4 and 13.3 microns ($750\text{--}4100\text{ cm}^{-1}$) with a maximum optical path difference of ± 25 cm (unapodized resolution $\sim 0.02\text{ cm}^{-1}$). The satellite also features a dual spectrograph known as MAESTRO with wavelength coverage 280-1000 nm and resolution 1-2 nm. A pair of filtered CMOS detector arrays takes images of the sun at 0.525 and 1.02 nm.

The measurement technique used for the mission is solar occultation, the geometry of which is depicted in Fig. 1.

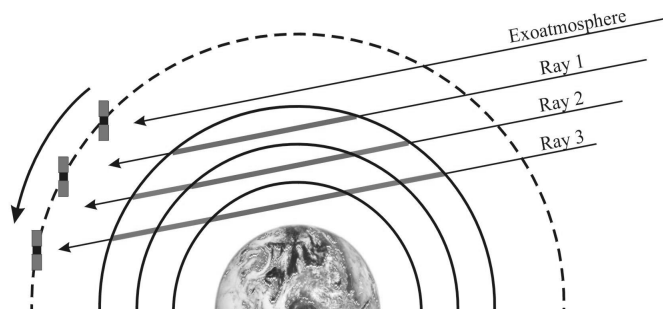


Fig. 1: Solar occultation

*cboone@uwaterloo.ca; phone (519) 888-4567 x6383; fax (519) 746-0435; <http://www.ace.uwaterloo.ca>; Department of Chemistry, University of Waterloo, Waterloo, Ontario, Canada, N2L 3G1

Over the course of an occultation event (i.e., a sunrise or a sunset in the satellite's frame of reference), the instruments take a series of measurements, where each measurement corresponds to a different ray path of sunlight through the Earth's atmosphere. Exoatmospheric measurements (solar measurements with no intervening atmosphere) are used as reference spectra, making the ACE instruments self-calibrating.

2. INSTRUMENTAL LINESHAPE

In order to obtain quantitative results from the FTS instrument on the ACE satellite, it is imperative to have an accurate representation of the instrumental lineshape (ILS). If one includes the effects of a finite scan and self apodization effects from the field of view,⁵ the calculated signal does not match well with the measurements, as seen in Fig. 2. Note that these are merely representative examples from many lines included in the fit. There are clearly self apodization effects in the spectrum beyond the normal field of view effects. One possible source of the self-apodization is modulation efficiency effects,⁶ i.e., increased losses in modulation efficiency at larger optical path differences during the FTS scan.

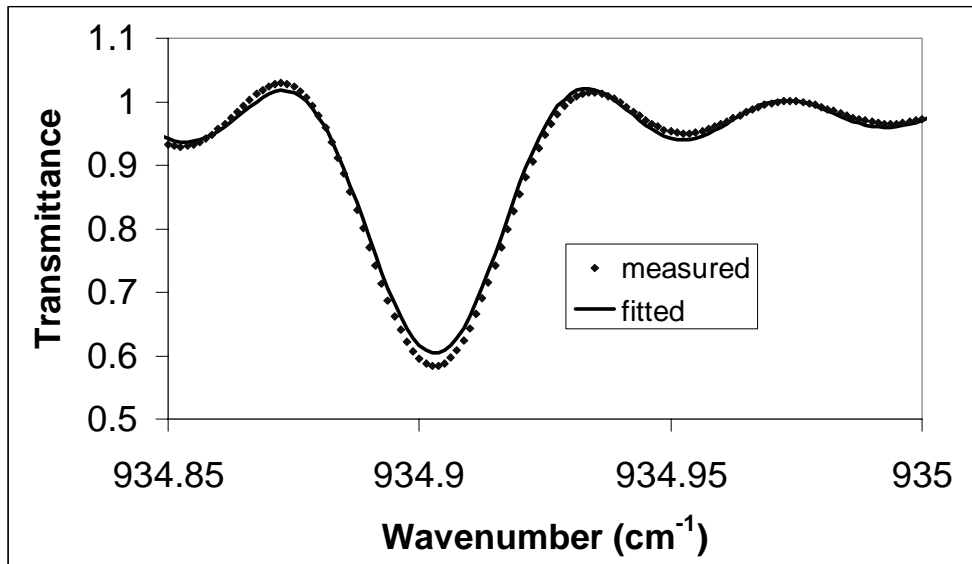


Fig. 2a: CO₂ fitting results, lower end of ACE wavenumber range, only including field of view effects on the ILS. Occultation ss2754, tangent height 22.5 km.

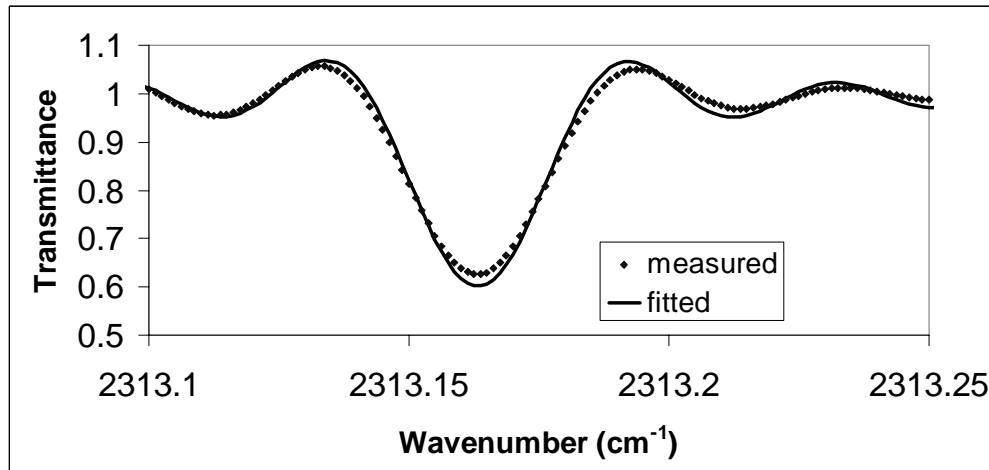


Fig. 2b: CO₂ fitting results, middle of ACE wavenumber range, only including field of view effects on the ILS. Occultation ss2754, tangent height 90 km.

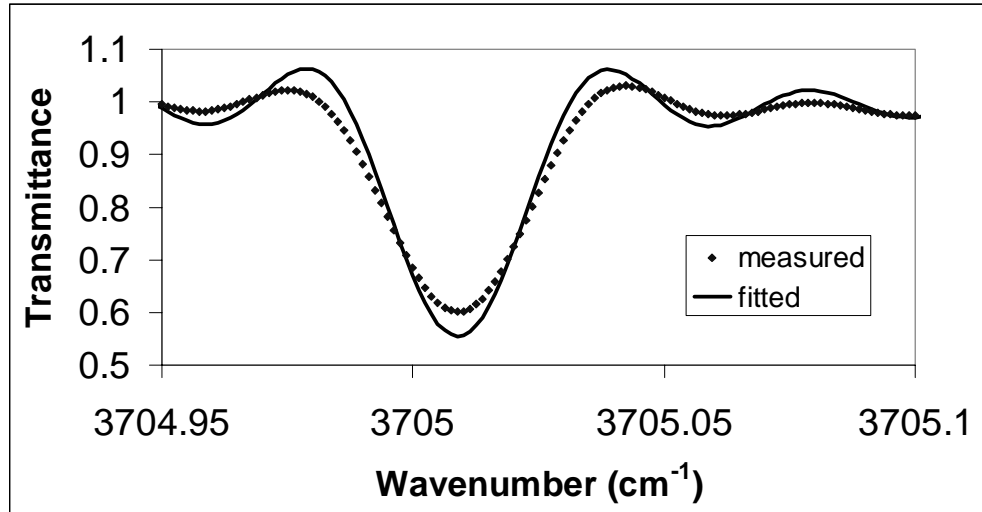


Fig. 2c: CO₂ fitting results, upper end of ACE wavenumber range, only including field of view effects on the ILS. Occultation ss2754, tangent height 90 km. The discrepancy increases significantly with increasing wavenumber.

In the absence of self-apodization effects the ILS for an FTS would be a pure sinc function, a consequence of the finite path difference of the FTS scan. The side lobes in the signal in Fig. 2 arise from this instrumental effect. The Fourier transform of the ideal sinc function to obtain is called the modulation function (a rectangular function). To account for self-apodization effects, one multiplies the modulation function by a peaked function. For the field of view effects, the peaked function is the central portion of another sinc function. The modulation function for the ACE-FTS when only accounting for field of view effects is shown in Fig. 3 (labelled “fov only”). The additional self-apodization is accounted for by multiplying by another peaked function. The function chosen was the following:

$$e^{\alpha_1 x^2 + \alpha_2 |x|^3 + \alpha_3 x^4},$$

where x is the path difference in cm and α_i are empirical parameters determined by performing a nonlinear least squares fit to the spectra. Only high altitude spectra were used in the determination of these parameters to avoid the complication of pressure broadening that would occur at lower altitudes. The resultant modulation function with the additional self-apodization effects (labelled “adjusted”) is also shown in Fig. 3.

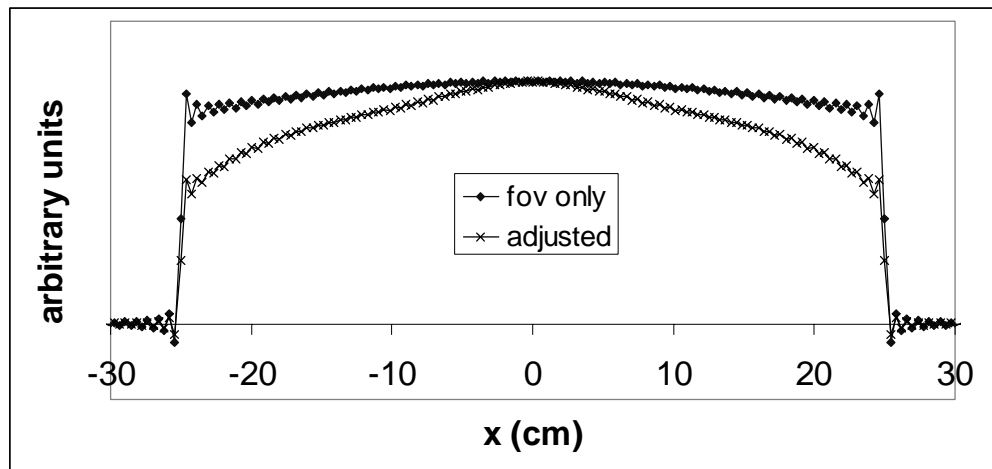


Fig. 3: ACE-FTS modulation function near 2400 cm⁻¹. The curve labelled “fov only” would be the result if field of view effects were the only contribution to self-apodization. The curve labelled “adjusted” is the empirical curve accounting for additional sources of self apodization.

There is little indication of asymmetry in the ACE-FTS lines, and so the phase (the imaginary part) of the modulation function was assumed to be zero. Linear variations as a function of wavenumber were assumed for each of the empirical parameters. The ILS was stable enough that a single set of parameters was determined for use with all occultations, and the set of parameters has proven to be usable for occultations spanning more than a month. Longer term changes in the ILS still need to be investigated.

The fitting results greatly improve with the empirical ILS. The results with the new ILS are shown in Fig. 4 for the same example shown in Fig. 2. As a quality test, this occultation was not included in the determination of the empirical ILS parameters.

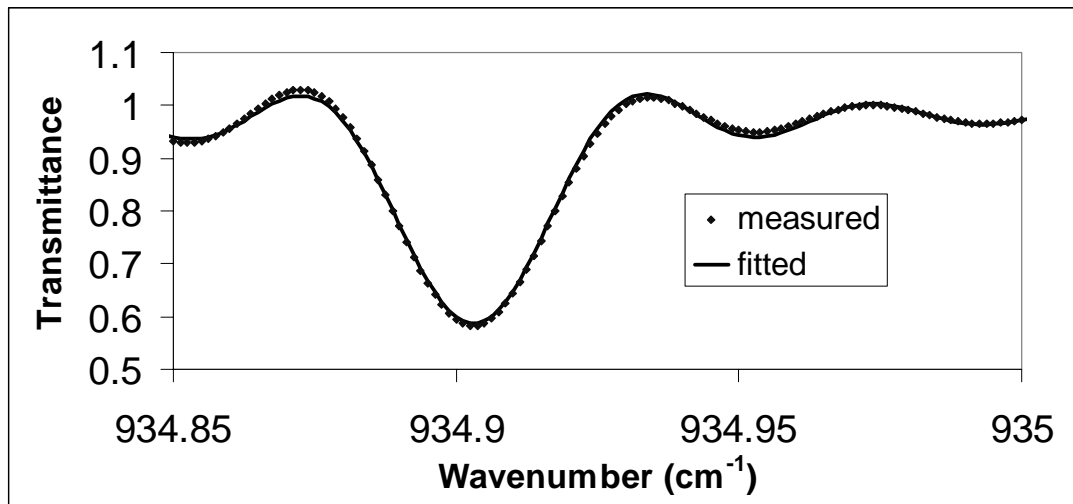


Fig. 4a: CO₂ fitting results using empirical ILS, low ACE cm⁻¹. Occultation ss2754, tangent height 22.5 km.

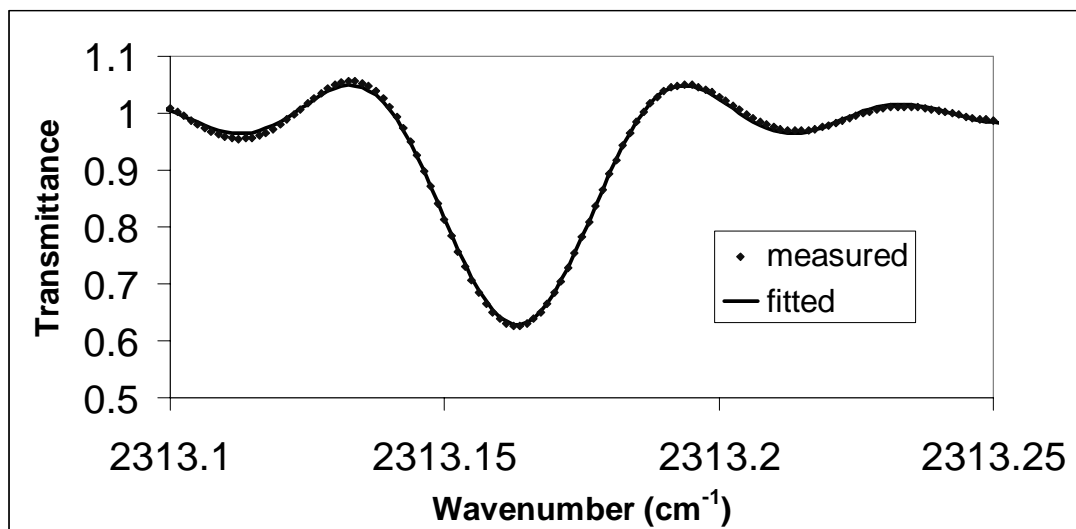


Fig. 4b: CO₂ fitting results using empirical ILS, central ACE cm⁻¹. Occultation ss2754, tangent height 90 km.

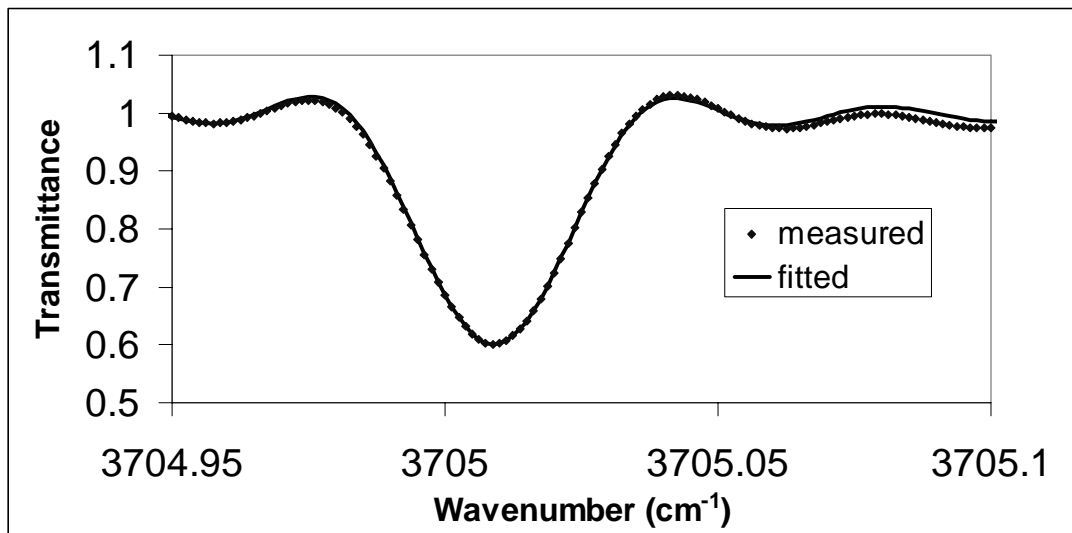


Fig. 4c: CO₂ fitting results using empirical ILS, high ACE cm⁻¹. Occultation ss2754, tangent height 90 km.

3. RESULTS

The analysis approach used for ACE-FTS data was described in a previous SPIE meeting proceedings.⁷ Briefly, the temperature and pressure profiles of the atmospheric region being measured are determined through analysis of CO₂ absorption features. The “poor pointing knowledge approach” described in Reference 7 is currently being used while we determine the best way to employ pointing information from the satellite sensors. Once pressure and temperature have been retrieved, the volume mixing ratio profiles of various molecules are then retrieved. The fourteen baseline molecules for the mission are O₃, H₂O, CH₄, N₂O, CO, NO, NO₂, HCl, HF, HNO₃, N₂O₅, ClONO₂, CFC-11, and CFC-12.

The results for the fourteen ACE baseline molecules are shown and compared for two occultations that occurred close to the same geographic location, but were separated by just over a month. The first occultation is labelled ss2754 and was measured on February 15th, 2004. The latitude of the measurement was ~65.5° North, and the longitude was ~ -82°. The second occultation is labelled ss3271 and was measured on March 21st, 2004. The latitude was ~64° N, and the longitude was ~ -85°. Interesting atmospheric effects can take place in the extreme north during spring, and so it is instructive to see what the passage of a month during this potentially volatile season does to the profiles of the ACE baseline molecules.

The retrieved temperature profiles are shown in Fig. 5. The February occultation, ss2754, is much cooler in the 30 km altitude region, but is not cold enough for the formation of polar stratospheric clouds (which occurs for temperatures below about 195 K).

Fig.6 shows the retrieval results for H₂O. There is much less water at higher altitudes for the occultation in February (ss2754), which could be due to descent of the polar air mass associated with the Arctic vortex. There is also reduced water between 18 and 30 km for ss2754. The “dehydration” in this altitude region is anti-correlated with increased levels of CH₄ and N₂O, as seen in Figs. 7 and 8, respectively. The profiles for CH₄ and N₂O have reduced levels at higher altitudes for ss2754, consistent with descent of the polar air mass. CH₄ and N₂O exhibit strong correlation, as expected for these two long-lived “tracer” molecules.

In Figs. 9 and 10, CO and NO in ss2754 are enhanced relative to ss3271 in the altitude range 50 to 80 km, possibly due to the descent of CO- and NO-enriched air.

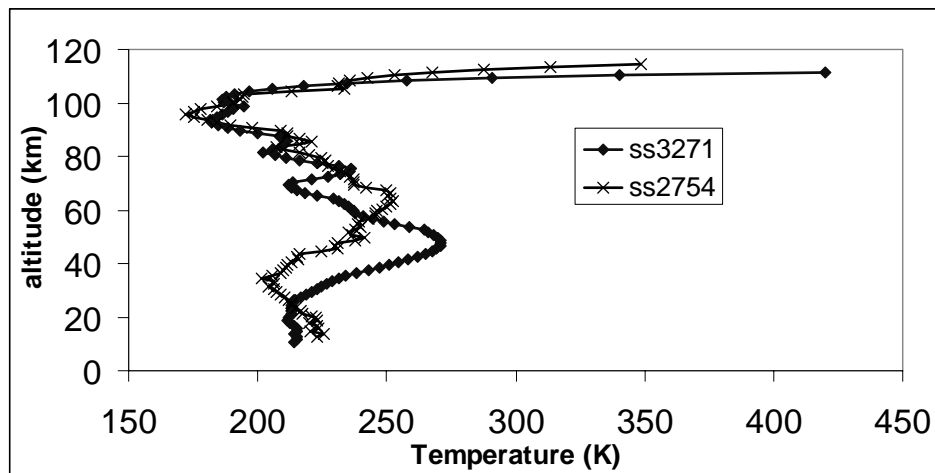


Fig. 5: Retrieved temperature profiles

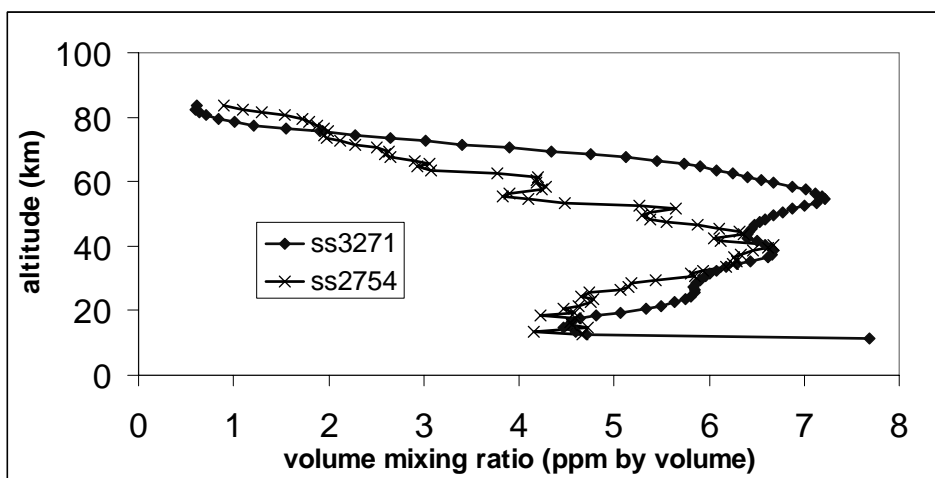


Fig. 6: H₂O retrievals

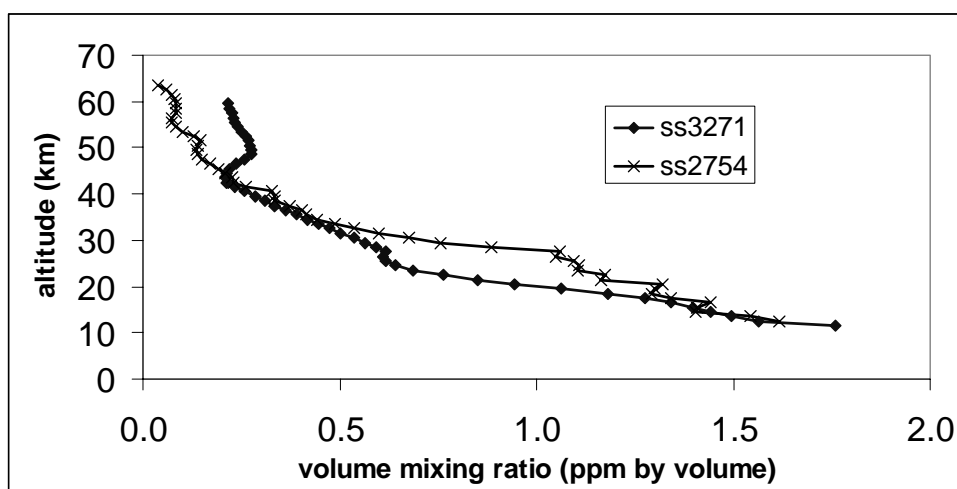


Fig. 7: CH₄ retrievals

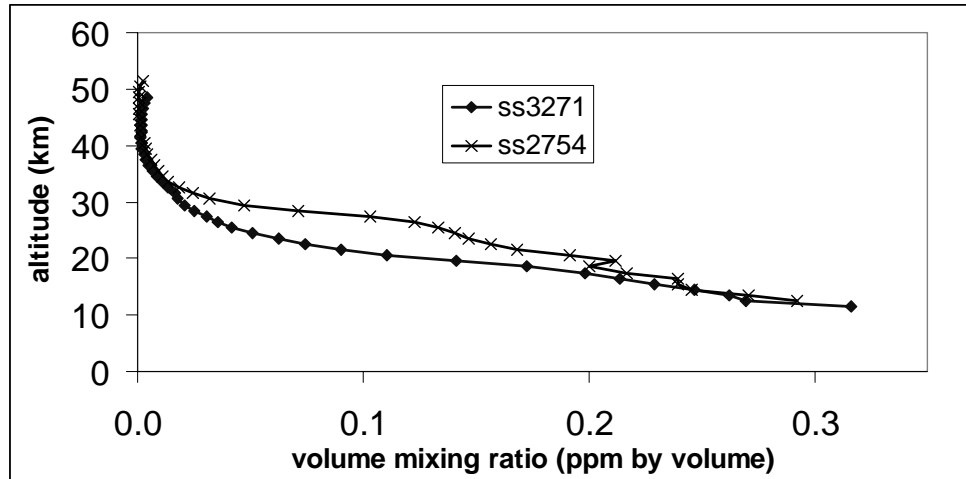


Fig. 8: N_2O retrievals

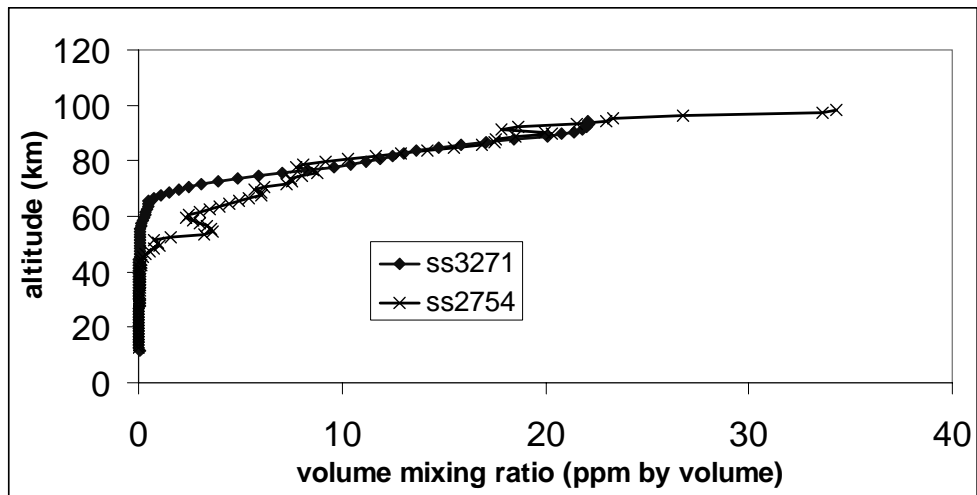


Fig. 9: CO retrievals

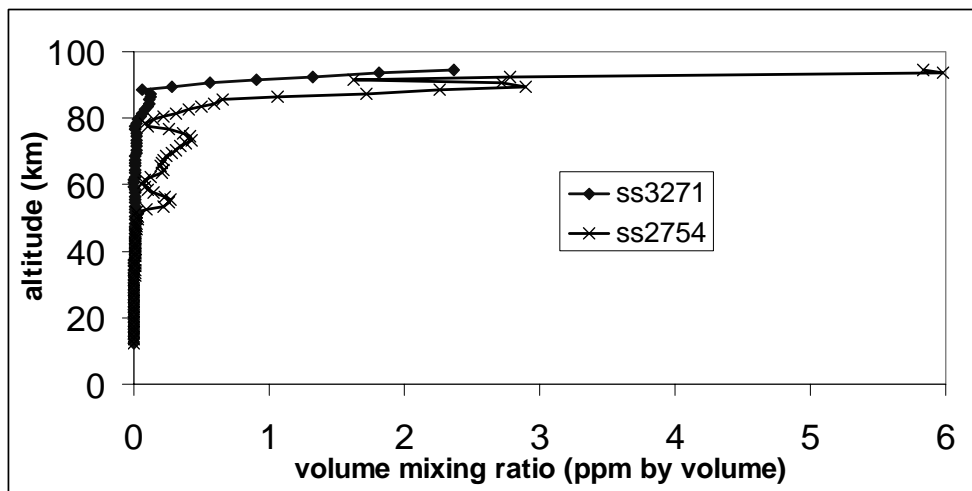


Fig. 10: NO retrievals

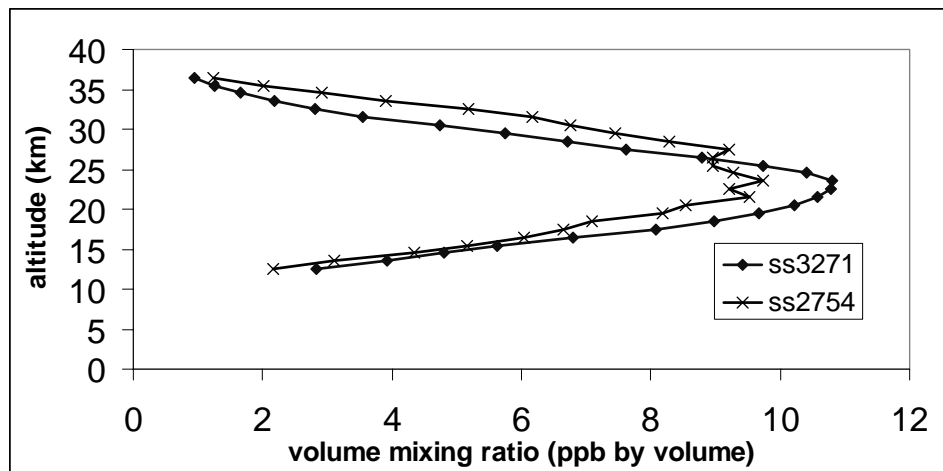


Fig. 11: HNO₃ retrievals

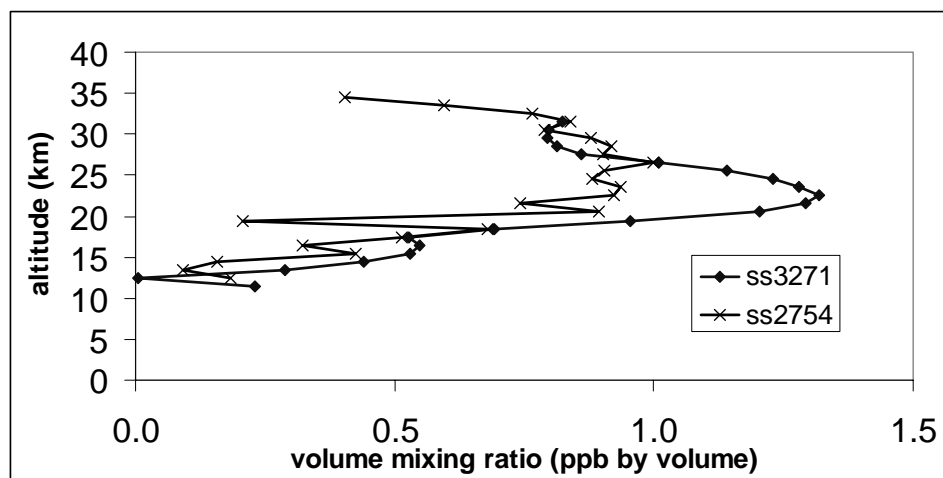


Fig. 12: ClONO₂ retrievals

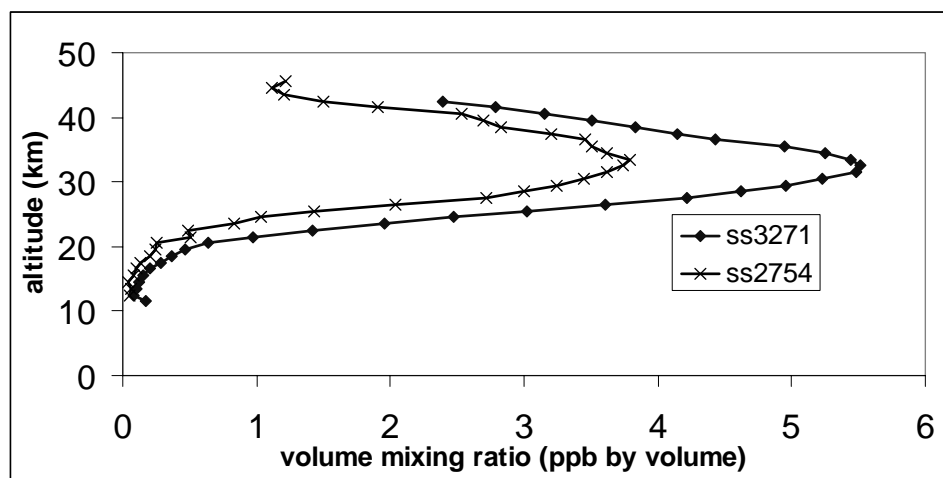


Fig. 13: NO₂ Retrievals

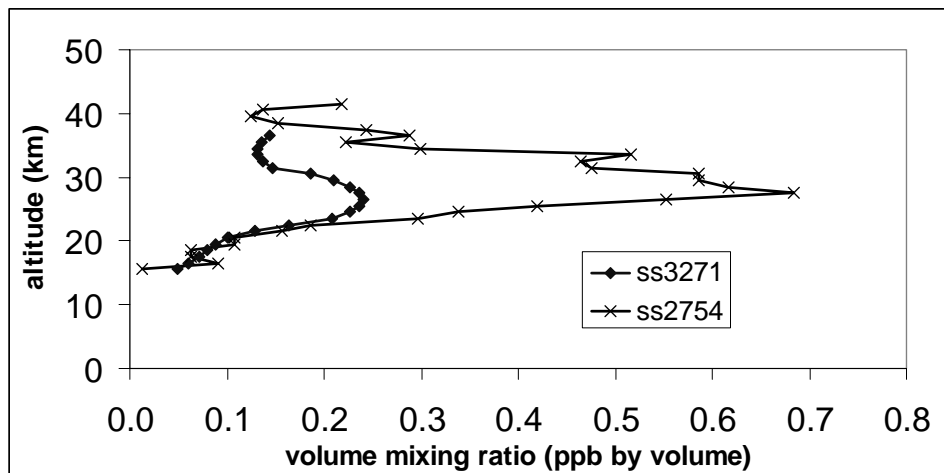


Fig. 14: N_2O_5 retrievals

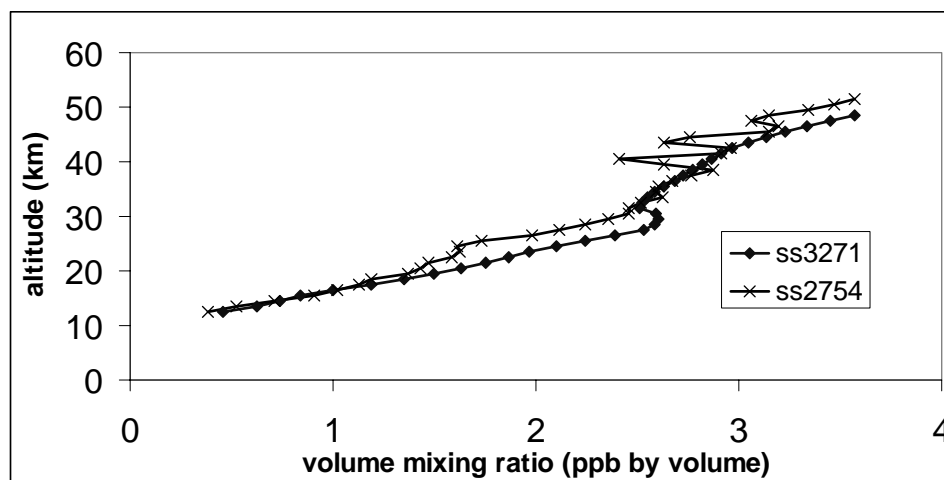


Fig. 15: HCl retrievals

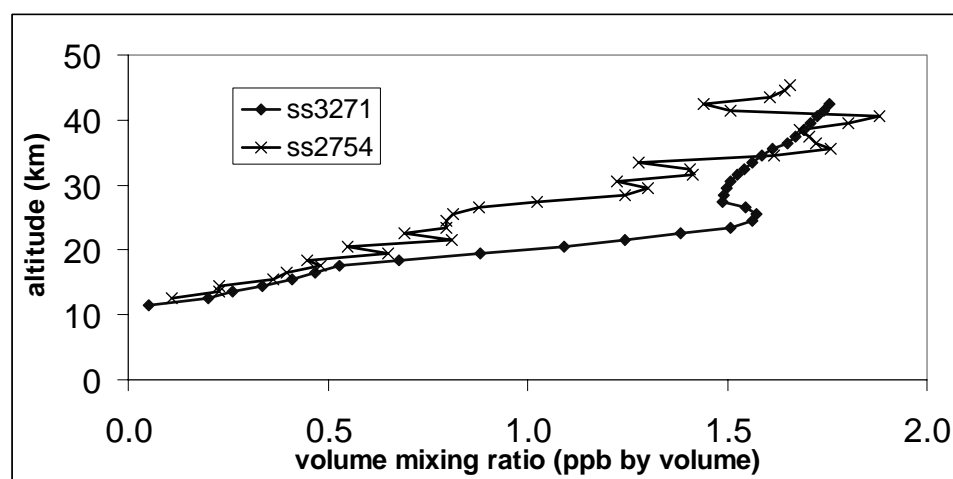


Fig. 16: HF retrievals

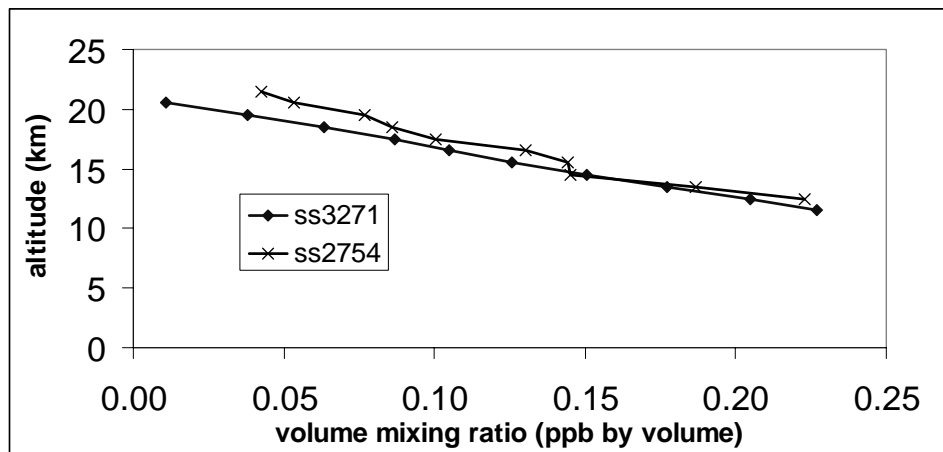


Fig. 17: CCl₃F (CFC-11) retrievals

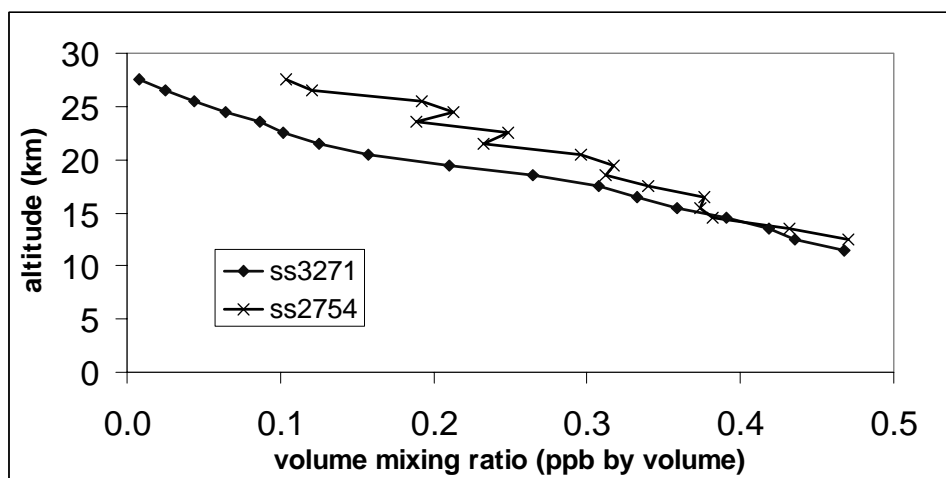


Fig. 18: CCl₂F₂ (CFC-12) retrievals

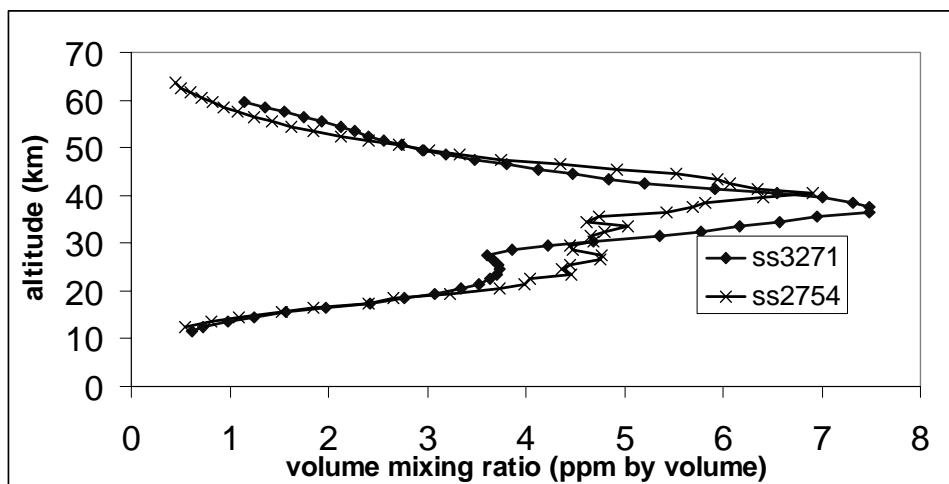


Fig. 19: O₃ retrievals

The profiles for HNO_3 and ClONO_2 in Figs. 11 and 12, respectively, indicate some reduction in the levels of these constituents for ss2754 compared to ss3271. Significant polar stratospheric cloud formation would entail strong reduction of these two molecules; the slight decline in HNO_3 levels for ss2754 suggests that there was little polar stratospheric cloud activity during the actual observation, as is expected for the observed temperatures. The higher levels of ClONO_2 in ss3271 could indicate that there was polar stratospheric cloud activity sometime during the winter.

There was significant nitrogen-constituent chemistry occurring, as evinced by the large differences in NO_2 and N_2O_5 in Figs. 13 and 14, respectively.

As was the case for H_2O , the behavior of HCl and HF (Figs. 15 and 16, respectively) in the 18 to 30 km altitude region is anti-correlated with the behavior of the “tracer” species CH_4 and N_2O . The CFCs (shown in Figs. 17 and 18), on the other hand, are correlated with CH_4 and N_2O .

Finally, the profiles for O_3 in Fig. 19 show some interesting structure. In order to properly model what is happening with O_3 , it is necessary to consider both transport effects and chemistry effects. However, judging from these two “snapshots,” it would seem that there was not a major loss of ozone in the Arctic during spring 2004.

ACKNOWLEDGMENTS

Thanks to the Canadian Space Agency and to NSERC for funding.

REFERENCES

1. D.J. Wardle, J.B. Kerr, C.T. McElroy, and D.R. Francis, eds., *Ozone Science: A Canadian Perspective on the Changing Ozone Layer*, Environment Canada, 1997.
2. J.S. Levine, *Global Biomass Burning: Atmospheric, Climatic, and Biospheric Implications*, MIT Press, 1991.
3. D.T. Shindell, D. Rind, and P. Lonergan, “Increased polar stratospheric ozone losses and delayed eventual recovery owing to increased greenhouse gas concentrations,” *Nature*, **392**, pp 589, 1998.
4. Intergovernmental Panel on Climate Change, *Climate Change 2001: The Scientific Basis*, World Meteorological Organization, Geneva, 2001.
5. P.R. Griffiths and J.A. de Haseth, *Fourier Transform Infrared Spectrometry*, Wiley, New York, 1986.
6. F. Hase, T. Blumenstock and C. Paton-Walsh, “Analysis of instrumental line shape of high-resolution FTIR-spectrometers using gas cell measurements and a new retrieval software”, *Applied Optics*, **38**, pp 3417-3422, 1999.
7. C. Boone and P. Bernath, “Pressure/temperature and volume mixing ratio retrievals for the Atmospheric Chemistry Experiment”, *Proceedings of SPIE*, **4814**, pp 50-61, 2002.